Mixed Convection Effects in Cavities with Oscillating Boundaries

Monique Soriano Vital da Silva[♦] **& José Carlos César Amorim**
Department of Mechanical and Materials Engineering
Instituto Militar de Engenharia
22290-270 – Rio de Janeiro – RJ
monique@lmt.coppe.ufrj.br, jcamorim@ime.eb.br

Albino José Kalab Leiroz[♣]
Department of Mechanical Engineering – POLI/COPPE
Universidade Federal do Rio de Janeiro
Caixa Postal 68503 - Rio de Janeiro – RJ – 21945-970
leiroz@ufrj.br

Abstract: *The transient evolution of the flow and temperature fields inside two-dimensional cavities with inwards oscillating wall is discussed in the present work. The existence of openings in the cavity wall is considered. The flow governing equations are solved using a Vorticity-Stream Function formulation. Appropriate stream-function boundary conditions are used to describe the openings along the upper wall and the oscillation wall movement. Vorticity values along the cavity solids boundaries and the openings are solved by an iterative solution method. Density variations are considered by the use of Boussinesq approximation. Initially, analytical transformations are used to obtain a stationary solution domain and to cluster points near the upper wall. The transformed governing equations are discretized using an implicit Finite-Difference scheme. The resultant algebraic system is solved by an iterative solution method with sub-relaxation and local error control. The parametric study is presented based on the Reynolds, Prandtl and Grashof numbers influence on the transient evolution of the flow and temperature fields inside the cavity. Obtained results are compared with pure forced convection data showing the influence of density variation on the evolution of flow and temperature fields.*

Keywords*: Cavity Flow, Mixed Convection, Numerical Methods and Grid Generation.*

1. Introduction

Flows within cavities with moving boundaries are commonly used for studies of basic fluid mechanics phenomena. Different flow structures associated with boundary layers and recirculation zones can be found in a yet simple geometry. Besides fundamental studies, cavity flows are related with important industrial applications that include the cooling of electronic equipment and building thermal insulation. The studies of flow field in cavities with openings through which mass is exchanged with the surroundings is of particular interest for applications in alternative engines and compressors.

Mixed convection in open cavities is numerically studied for different configurations considering vertical, horizontal and inclined external flows (Khanafer, 2002). A parametric study on the nondimensional parameters governing the phenomena, such as Reynolds and Grashof numbers and the cavity aspect ratio, is conducted. Results show that the flows associated with the opening can be used to thermally insulate the cavity from the surroundings. Low Grashof results indicate low mean Nusselt values for opening flow angle between 45^o and 90^o. The existence of a critical Reynolds number for which the opening flow becomes dominant over the natural convection effects is observed for the 90^o angle (Khanafer, 2002).

The numerical study of the mixed convection effects during the hydrodynamic removal of contaminants in a cavity inside a duct uses the solution of the transient Navier-Stokes equations coupled with the energy conservation equation (Fang, 2002). The mixed convection effects on the temporal evolution of the flow field and on the contaminants removal from the cavity are discussed. Results indicate a strong dependence of the flow field structure and the removal efficiency on the Grashof number due to the interaction between the external duct flow and the buoyancy force generated by the heating source.

Flow in deep cavities induced by moving boundaries and temperature gradients are also analyzed for a wide range of Gr/Re^2 (Prasad, 1996). The nondimensional parameters are defined using the upper wall velocity, the vertical temperature difference and the cavity depth as characteristic values for velocity, temperature and length, respectively. Liquid crystals are used for flow visualization. Heat flux measurements along the lower walls are also performed. Results show that the flow pattern near the lower wall is unaffected by the cavity aspect ratio and imposed temperature gradient and that weak dependence of the heat transfer coefficient on the Gr/Re^2 values (Prasad, 1996).

♦ Present Address: Department of Mechanical Engineering – COPPE, Universidade Federal do Rio de Janeiro.
♣ Author to whom correspondence should be addressed.

The numerical solution for the flow and temperature fields within cavities within two-dimensional cavities with the lower wall in oscillating harmonic displacement. Openings on the upper wall are also considered. The flow through the upper wall openings is controlled by the lower wall movement. Density variations are considered using the Boussinesq approximation and the flow field is described using a vorticity-stream function formulation. Analytical coordinate transformations are used to obtain a stationary computational domain and control the grid point distribution.

2. ANALYSIS

A sketch of the solution domain is show in Fig. 1, which also shows the Cartesian system of coordinates used and the cavity principle dimensions. The lower wall movement is described by an arbitrary function $h(t)$. The upper wall openings allow for mass flow between the cavity and the surroundings. Due to the incompressible flow assumption used in the present work, the fluid velocity within the openings depends on the lower wall velocity - $\dot{h}(t)$ - and the cavity geometry.

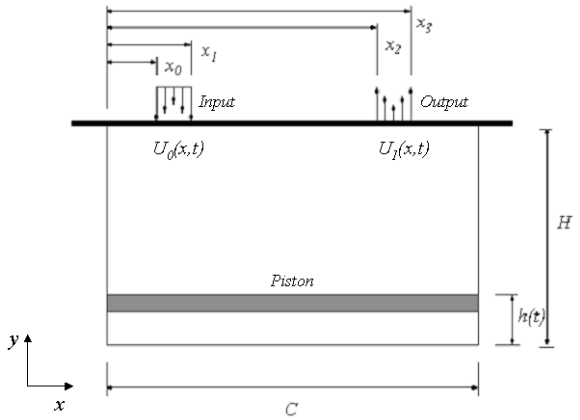

Figure 1. Physical domain, principle dimensions and coordinate system.

Neglecting viscous dissipation effects, considering density variation through the Boussinesq approximation and the remaining thermophysical properties as constants, the mixed convection governing equations are written in nondimensional form as

$$r_a \frac{\partial u_x}{\partial x} + \frac{\partial u_y}{\partial y} = 0 \tag{1}$$

$$\frac{\partial u_x}{\partial t} + u_x r_a \frac{\partial u_x}{\partial x} + u_y \frac{\partial u_x}{\partial y} = -r_a \frac{\partial p}{\partial x} + \frac{1}{Re}\left(r_a^2 \frac{\partial^2 u_x}{\partial x^2} + \frac{\partial^2 u_x}{\partial y^2} \right) \tag{2}$$

$$\frac{\partial u_y}{\partial t} + u_x r_a \frac{\partial u_y}{\partial x} + u_y \frac{\partial u_y}{\partial y} = -\frac{\partial p}{\partial y} + \frac{1}{Re}\left(r_a^2 \frac{\partial^2 u_y}{\partial x^2} + \frac{\partial^2 u_y}{\partial y^2} \right) + r_a \frac{Gr}{Re^2} \frac{\partial \theta}{\partial x} \tag{3}$$

$$\frac{\partial \theta}{\partial t} + u_x r_a \frac{\partial \theta}{\partial x} + u_y \frac{\partial \theta}{\partial y} = \frac{1}{Re\, Pr}\left(r_a^2 \frac{\partial^2 \theta}{\partial x^2} + \frac{\partial^2 \theta}{\partial y^2} \right) \tag{4}$$

Boundary conditions are written, for lower wall movement in upward movement as

$$u_x = 0, \quad u_y = 0, \quad -r_a \frac{\partial \theta}{\partial x} + Bi\theta = Bi\theta_\infty ; \quad x = 0, \quad h(t) < y < 1, \quad \dot{h}(t) > 0 \tag{5}$$

$$u_x = 0, \quad u_y = 0, \quad \frac{\partial \theta}{\partial y} + Bi\theta = Bi\theta_\infty ; \quad 0 < x < x_2, \quad y = 1, \quad \dot{h}(t) > 0 \tag{6}$$

$$u_x = 0, \quad u_y = U_1(x,t), \quad \frac{\partial \theta}{\partial y} = 0 ; \quad x_2 < x < x_3, \quad y = 1, \quad \dot{h}(t) > 0 \tag{7}$$

$$u_x = 0, \quad u_y = 0, \quad \frac{\partial \theta}{\partial y} + Bi\theta = Bi\theta_\infty ; \quad x_3 < x < 1/r_a, \quad y = 1, \quad \dot{h}(t) > 0 \tag{8}$$

$$u_x = 0, \quad u_y = 0, \quad r_a \frac{\partial \theta}{\partial x} + Bi\theta = Bi\theta_\infty ; \quad x = 1/r_a, \quad h(t) < y < 1, \quad \dot{h}(t) > 0 \tag{9}$$

$$u_x = 0, \quad u_y = \dot{h}(t), \quad -\frac{\partial \theta}{\partial y} + Bi\theta = Bi\theta_\infty ; \quad 0 < x < 1/r_a, \quad y = h(t), \quad \dot{h}(t) > 0 \tag{10}$$

and for downward movement of the lower wall

$$u_x = 0, \quad u_y = 0, \quad -r_a \frac{\partial \theta}{\partial x} + Bi\theta = Bi\theta_\infty ; \quad x = 0, \quad h(t) < y < 1, \quad \dot{h}(t) < 0 \tag{11}$$

$$u_x = 0, \quad u_y = 0, \quad \frac{\partial \theta}{\partial y} + Bi\theta = Bi\theta_\infty ; \quad 0 < x < x_2, \quad y = 1, \quad \dot{h}(t) < 0 \tag{12}$$

$$u_x = 0, \quad u_y = U_0(x,t), \quad \theta = 0 ; \quad x_2 < x < x_3, \quad y = 1, \quad \dot{h}(t) < 0 \tag{13}$$

$$u_x = 0, \quad u_y = 0, \quad \frac{\partial \theta}{\partial y} + Bi\theta = Bi\theta_\infty ; \quad x_3 < x < 1/r_a, \quad y = 1, \quad \dot{h}(t) < 0 \tag{14}$$

$$u_x = 0, \quad u_y = 0, \quad r_a \frac{\partial \theta}{\partial x} + Bi\theta = Bi\theta_\infty ; \quad x = 1/r_a, \quad h(t) < y < 1, \quad \dot{h}(t) < 0 \tag{15}$$

$$u_x = 0, \quad u_y = \dot{h}(t), \quad -\frac{\partial \theta}{\partial y} + Bi\theta = Bi\theta_\infty ; \quad 0 < x < 1/r_a, \quad y = h(t), \quad \dot{h}(t) < 0 \tag{16}$$

with $U_0(x,t)$ e $U_1(x,t)$ defined by the lower wall velocity and the cavity geometry using the incompressible flow assumption.

Initial conditions, corresponding to stagnant and isothermal fluid, are written as

$$u_x = 0, \quad u_y = 0, \quad \theta = 0; \quad 0 < x < 1/r_a, \quad h(t) \le y \le 1 \tag{17}$$

The nondimensional variables are defined using the cavity width C, the cavity height H as characteristic length in the x and y directions, respectively and the maximum value of the lower wall velocity $\dot{h}_{max}$ as characteristic velocity. The nondimensional temperature is defined using the difference between the inlet fluid temperature T_e and the characteristic lower wall temperature T_f. The nondimensional parameters are defined as

$$r_a = \frac{H}{C}, \qquad x = \frac{x^*}{C}, \qquad y = \frac{y^*}{H}, \qquad t = \frac{t^* \dot{h}_{max}}{H}, \qquad u_x = \frac{u_x^*}{\dot{h}_{max}}, \qquad u_y = \frac{u_y^*}{\dot{h}_{max}}$$

$$\theta = \frac{T^* - T_e}{T_f - T_e}, \qquad Re = \frac{H \dot{h}_{max}}{\nu}, \qquad Pr = \frac{\nu}{\alpha}, \qquad Gr = \frac{g \beta H^3}{\upsilon^2}(T_f - T_e), \qquad Bi = \frac{h H}{k} \tag{18}$$

where r_a, Re, Pr, Gr and Bi are the cavity aspect ratio, the Reynolds, Prandtl, Grashof and Biot numbers, respectively.

In order to decouple the solution for the velocity and pressure fields and reduced to number of equation being simultaneously solved, the flow governing equation are rewritten in Vorticity-Stream Function Formulation as

$$\frac{\partial \omega}{\partial t} + u_x r_a \frac{\partial \omega}{\partial x} + u_y \frac{\partial \omega}{\partial y} = \frac{1}{Re}\left(r_a^2 \frac{\partial^2 \omega}{\partial x^2} + \frac{\partial^2 \omega}{\partial y^2} \right) + r_a \frac{Gr}{Re^2} \frac{\partial \theta}{\partial x} \tag{19}$$

$$r_a^2 \frac{\partial^2 \psi}{\partial x^2} + \frac{\partial^2 \psi}{\partial y^2} = -\omega \tag{20}$$

Vorticity (ω) and stream-function (ψ) are defined in terms of the cartesian velocity components, respectively, as

$$r_a \frac{\partial u_y}{\partial x} - \frac{\partial u_x}{\partial y} = \omega \tag{21}$$

$$u_x = \frac{\partial \psi}{\partial y}, \quad u_y = -\frac{\partial \psi}{\partial x} \tag{22}$$

The dimensional and nondimensional vorticity and stream-function are related by

$$\omega = \frac{\omega^* \dot{h}_{max}}{H} \qquad \psi = \frac{\psi^*}{H \dot{h}_{max}} \tag{23}$$

The stream function boundary conditions are obtained from the appropriate integration of Eq. (22), as

$$\psi = 0\,; \quad x = 0, \quad h(t) < y < 1 \tag{24}$$

$$\psi = g(x,t)\,; \quad 0 < x < 1/r_a, \quad y = 1 \tag{25}$$

$$\psi = \psi_3(x,y,t)\,; \quad x = 1/r_a, \quad h(t) < y < 1 \tag{26}$$

$$\psi = \psi_4(x,y,t)\,; \quad 0 < x < 1/r_a, \quad y = h(t) \tag{27}$$

where

$$g(x,t) = \begin{cases} 0, & 0 < x < x_i \\ \psi_0(x,1,t), & x_i < x < x_f \\ \psi_1(x,1,t), & x_f < x < 1/r_a \end{cases} \tag{28}$$

The choice of a stream function value at a given point of the cavity boundary and the velocity profile along the upper wall openings are required for the definition of the stream function boundary conditions. It is noteworthy that vorticity values along the solid walls are unknown and are calculated by an iterative solution procedure (Anderson et al., 1984).

The flow field initial conditions are written for the Vorticity- Stream function Formulation as

$$\psi = 0, \quad \omega = 0, \quad 0 \le x \le 1/r_a, \quad h(t) \le y \le 1 \tag{29}$$

3. NUMERICAL ASPECTS

Initially, a transformation of coordinates is introduced in order to allow for the solution of the governing equations within a stationary computational domain (Hoffman, 1992). The physical and computational variables are related by

$$t = \tau \tag{30}$$

$$y = [H - h(t)]\eta + h(t) \tag{31}$$

$$h = \frac{y - h(t)}{H - h(t)} \tag{32}$$

For the transformation described by Eqs. (30-31), the analytically obtained metrics are defined as

$$\tau_t = 1 \tag{33}$$

$$\tau_\eta = 0 \tag{34}$$

$$\eta_t = \frac{\dot{h}(t)[h(t) - H] + \dot{h}(t)[y - h(t)]}{[H - h(t)]^2} \tag{35}$$

$$\eta_y = \frac{1}{H - h(t)} \tag{36}$$

$$\eta_{yy} = 0 \tag{37}$$

In order to cluster points near the upper cavity wall, where high solution gradients are expected, another transformation of coordinates is introduced. The grid point clustering near the upper wall is obtained by

$$\eta = \frac{\beta\left(\frac{\beta+1}{\beta-1}\right)^{\zeta} - \beta}{1 + \left(\frac{\beta+1}{\beta-1}\right)^{\zeta}} \tag{38}$$

$$\zeta = \frac{ln\left(\frac{\beta+\eta}{\beta-\eta}\right)}{ln\left(\frac{\beta+1}{\beta-1}\right)} \tag{39}$$

where β is the clustering parameter (Hoffman, 1992). For the transformation described in Eq. (38), the metrics are also analytically obtained and defined as

$$\zeta_\eta = \frac{2 \cdot \beta}{\left(\beta^2 - \eta^2\right) \cdot ln\left(\frac{\beta+1}{\beta-1}\right)} \tag{40}$$

$$\zeta_{\eta\eta} = \frac{-2 \cdot (\beta + \eta)}{\left(\beta^2 - \eta^2\right)^2 \cdot ln\left(\frac{\beta+1}{\beta-1}\right)} \tag{41}$$

The governing equations – Eqs. (4,19-20) – are rewritten using the transformed variables τ and η and discretized using the BTCS Finite Difference scheme. The resulting system of algebraic equations is solved by a Gauss-Seidel subroutine with under-relaxation and local error control.

4. RESULTS

The results obtained from the computational procedure where initially validated using literature results for lid driven cavity and analytical results available for the temperature field for the limiting case of stagnant conditions.

For the present work, results where obtained for a *41x41* grid, considering $r_a = 1$, $\beta = 1.02$, $Re = 10$, $Pr = 1$, $Gr = 10^5$ and $Bi = 10^5$. An harmonic movement described by

$$h(t) = h_0\left[1 + sen(\alpha t)\right] \tag{42}$$

is considered for lower cavity wall. The initial lower wall position h_o equal to *0.1* is used. Results are shown for different lower wall positions. During the upward movement of the lower wall ($\dot{h} > 0$), the discharge valve remains open and the admission valve remains closed. As the lower wall moves downwards ($\dot{h} < 0$), the flow and temperature condition on the cavity openings are switched.

Stream function and temperature results are shown in Figs. 2 and 3, respectively, for different time intervals. Results depicted in Figs. 2a and 3a show flow patterns induced by the upward movement of the lower wall and a uniform temperature distribution within the cavity. As the temperature field develops, natural convection effects become stronger. Results in Fig. 2b show the existence of recirculation zones, represented by dashed lines as the lower wall is in downward motion and the admission valve is opened. The incoming and cooler flow is forced downward between the recirculation zones where warmer fluid is contained (Fig.3b). Results in Fig.2c show that the recirculation zones are weakened as the lower wall moves towards the upper wall. Results also show that the temperature of the fluid leaving the cavity through the discharge valve is at a lower temperature than the temperature near the cavity wall. Figures 2d show the increase of the recirculation zones as the lower wall moves downwards with at higher rate than in Fig 2b. When the lower wall changes direction ($\dot{h} = 0$), admission and discharge openings are close and the resulting flow pattern is shown in Fig. 2e. Two recirculation zones are present and, due to zero mean velocity, no forced convection is observed.

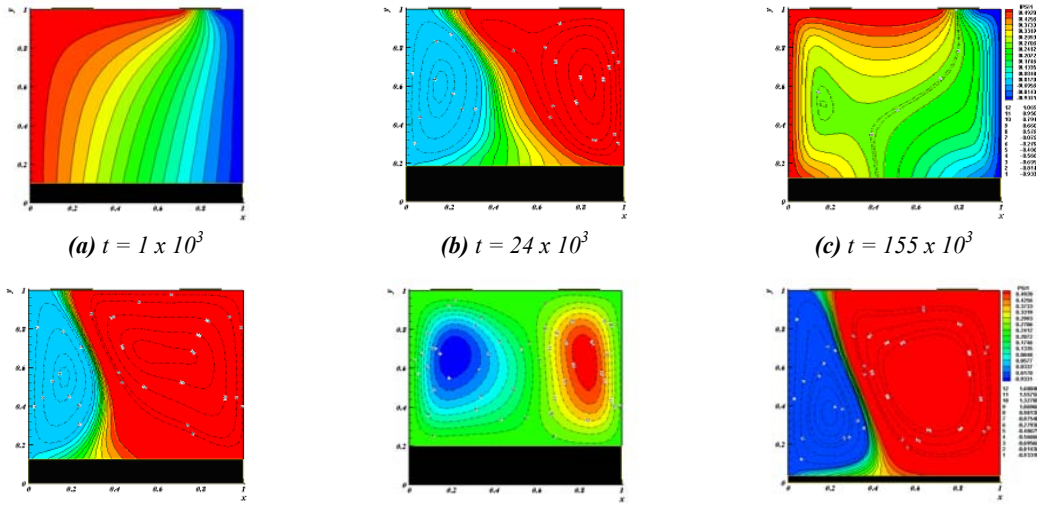

(a) $t = 1 \times 10^3$ ***(b)*** $t = 24 \times 10^3$ ***(c)*** $t = 155 \times 10^3$

(d) $t = 212 \times 10^3$ ***(e)*** $t = 288 \times 10^3$ ***(f)*** $t = 385 \times 10^3$

Figure 2. Flow Field for Stream Function - Cycle 1

Further results on the temporal evolution of the temperature field are shown in Fig. 3. During the initial times, a thin thermal boundary layer develops along the cavity walls and the process is diffusion controlled due to the small velocities (Fig.3a). As the lower wall moves upwards, the discharge opening is opened. Initially, the warmer fluid close to the solid boundary leaves the cavity followed by the cooler fluid originally on the cavity center (Fig.3b). As the lower wall moves towards the maximum height, the displacement rate is reduced and diffusion controlled heating of the cavity center is observed (Fig.3c).

The inlet valves opens as the lower cavity wall moves downwards as shown in Figs. (3d-3f). The thermal boundary layer associated with the vertical wall in $x = 0$ is affected by the incoming opening flow. As the velocity of the lower wall reaches a maximum at $y = 0.1$, the intensity of the recirculation zones increases and convective effects influence

the temperature distribution. The recirculation effect on the temperature distribution is observed from the differences between the results depicted in Figs. 3e and 3f.

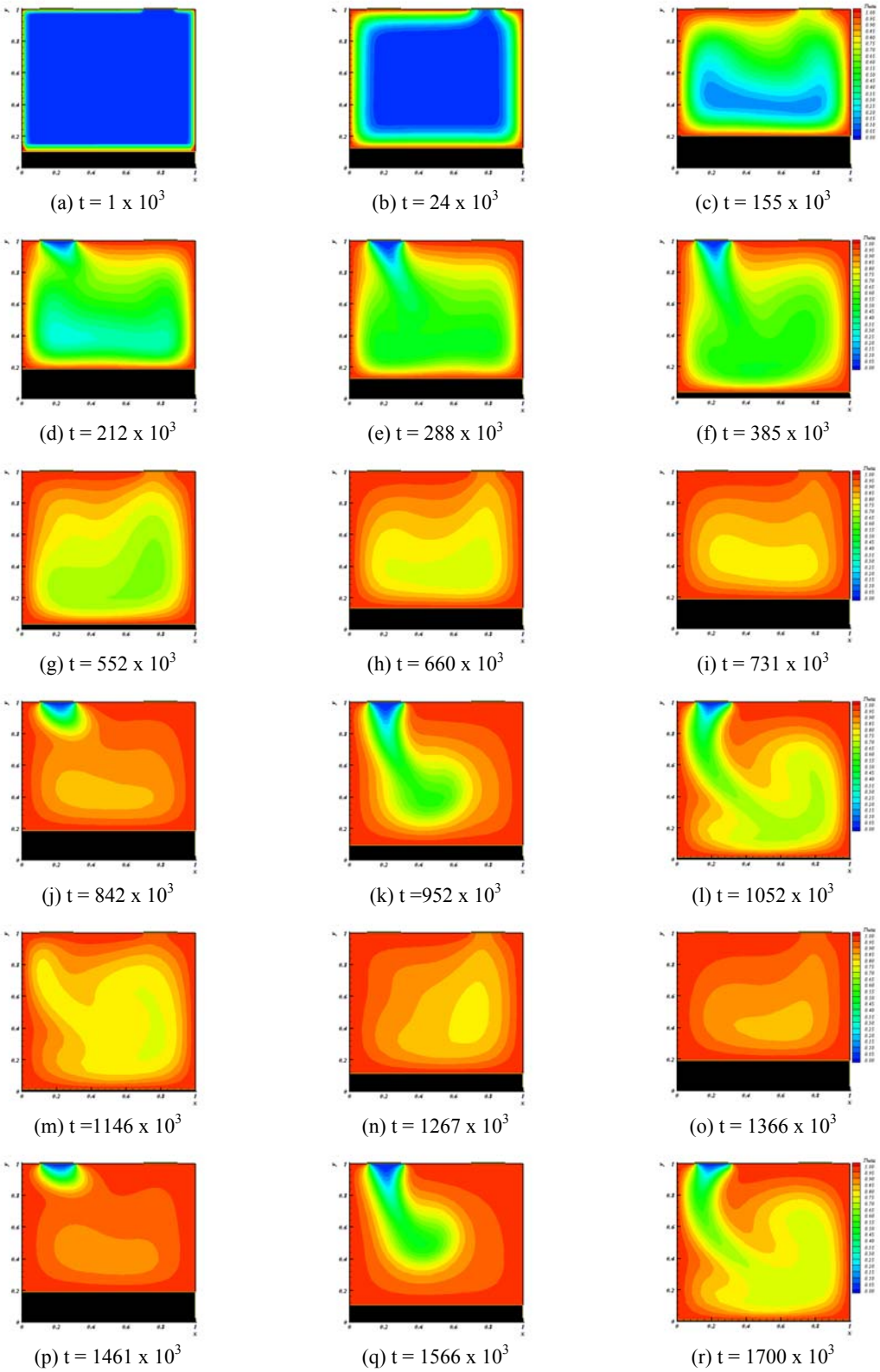

(a) t = 1 x 10^3 (b) t = 24 x 10^3 (c) t = 155 x 10^3

(d) t = 212 x 10^3 (e) t = 288 x 10^3 (f) t = 385 x 10^3

(g) t = 552 x 10^3 (h) t = 660 x 10^3 (i) t = 731 x 10^3

(j) t = 842 x 10^3 (k) t =952 x 10^3 (l) t = 1052 x 10^3

(m) t =1146 x 10^3 (n) t = 1267 x 10^3 (o) t = 1366 x 10^3

(p) t = 1461 x 10^3 (q) t = 1566 x 10^3 (r) t = 1700 x 10^3

Figure 3. Temperature Field for Mixed Convection,
Cycle 1 in (a)-(f), Cycle 2 in (g)-(l) e Cycle 3 in (m)-(r)

As the lower cavity wall moves upwards, the discharge valve opens and the temperature distribution is shown in Figs (3g-3i). The effect of the outgoing flow on the thermal boundary layer along the vertical wall on $x = 1$ is smaller than the effect of the incoming flow on the corresponding vertical wall on $x = 0$. Temperature results shown in Figs. (3g-3i) also also show that convective effects are less important due to weakening of the recirculation zones during upward lower wall movement. As the lower wall continues to cycle between $y = 0$ and $y = 0.2$ the temperature field evolves showing increasing convective effects as shown in Figs. (3j-3r).

5. CONCLUSIONS

The transient evolution of the velocity and temperature fields is discussed within square cavities with lower oscillating wall are discussed. Opening on the upper wall are considered in order to allow the study the influence of incoming and discharging flow on the velocity and temperature fields.

Results show that mixed convection effects are responsible for the existence of recirculation zones within the flow field. The recirculation zones are generated by the interaction between the incoming cooler fluid and the warmer cavity fluid.

6. ACKNOWLEDGEMENTS

The authors would like to acknowledge the financial support provided by *CNPq*. Computational resources where allocated by the Thermal Engines Laboratory from COPPE/UFRJ

7.REFERENCES

Anderson, D.A. et al., “Computational Fluid Mechanics and Heat Transfer”, New York: Hemisphere Publishing Corporation, 1984.

Fang, L., “Effect of Mixed Convection on Transient Hydrodynamic Removal of a Contaminant from a Cavity”, Int. Journal of Heat and Mass Transfer, v. 46, p. 2039-2049, 2003.

Khanafer, K. et al., “Mixed Convection Heat Transfer in Two-Dimensional Open-Ended Enclosures”, Int. Journal of Heat and Mass Transfer, v. 45, p. 5171-5190, 2002.

Prasad, A.K., Koseff, J.R., “Combined Forced and Natural Convection Heat Transfer in a Deep Lid-Driven Cavity Flow”, Int. J. Heat and Fluid Flow, v. 17, p. 460-467, 1996.